

SMALL SCALE EXPERIMENTAL TESTING TO VERIFY THE EFFECTIVENESS OF THE BASE ISOLATION AND TUNED MASS DAMPERS COMBINED CONTROL STRATEGY

L. Petti¹, G. Giannattasio², M. De Iuliis³

¹ Assistant Professor, Dept. of Civil Engineering, University of Salerno, Italy – Email: petti@unisa.it

² PhD student, Dept. of Civil Engineering, University of Salerno, Italy – Email: jionny203@yahoo.it

³ Research Assistant, Dept. of Civil Engineering, University of Salerno, Italy – Email: mdeiuliis@unisa.it

ABSTRACT :

This paper presents the most significant results obtained within a broad range of experimental tests aimed at evaluating both the effectiveness and robustness of the Base Isolation (BIS) and Tuned Mass Damper (TMD) combined control strategy (BIS&TMD). After a brief description of the experimental model set-up, the paper describes the identification procedures for the fixed base structure, the base isolated structure and the base isolated structure equipped with a mass damper system. The main experimental results, representing the dynamic response of a small-scale model to scaled recorded earthquake excitations, are later presented and discussed. Finally, the effectiveness and robustness of the combined control strategy is investigated by comparing the model's dynamic response, in particular the reduction in relative displacements and absolute accelerations due to the application of different mass damping systems are evaluated.

KEYWORDS: Base Isolation, Mass Damper, Hybrid Control, Experimental Test

1. INTRODUCTION

In the last few years, non-conventional aseismic strategies (seismic isolation, extra-structural energy dissipation...) have come about as innovative solutions both for the construction of new structures and retrofitting existing ones. Among these techniques, base isolation strategy has shown its high level of effectiveness in practical applications worldwide, and is widely considered to be a suitable solution to ensure both high safety levels, with regard to the risk of collapse resulting from rare seismic events, and high performances in the case of moderate and more frequent earthquakes.

As is well-known, the effectiveness of a base isolation system (BIS) depends on the filtering capacity of the range of frequencies where the earthquake energy is strongest. The BIS acts as a low-pass filter which allows for the passage of low-frequency seismic excitations and reduces the amplitude of signals with frequencies higher than the isolation system frequency (cutoff frequency). However, filtering action has, on occasions, to be applied to an unpredictable excitation having a frequency content of an aleatory nature. The first natural frequency can never shift out of the entire frequency range for any type of seismic excitation, therefore the BIS structures under certain conditions of excitation may suffer from very high displacements at the base.

In 1994, Palazzo and Petti proposed a new combined control system based on the application of mass damping on the isolation layer in a base isolation structure.

The idea of new hybrid systems, based on a combination of the Tuned Mass Damper strategy (TMD) and BIS, came from the observation that the responses of well-isolated systems are dominated by the first-modal contribution and that TMD is able to reduce solely that fundamental vibration mode. In fact TMD acts as a band-pass filter which only allows for the passage of those frequencies within a certain range. The objective is to protect the BIS from those excitation components close to the natural vibration frequency by controlling the amplitude of the fundamental modal contribution due to the satellite TMD action installed on the base isolation layer.

Within this context, the present paper aims to investigate mass damping effectiveness and robustness in reducing the relative seismic displacement at isolation level, and its effect on the dynamic behaviour of the superstructure by performing a broadly experimental approach to evaluate the dynamic response of a small-scale three degree of freedom model.

The experimental work has been divided into two phases: in the first phase model identification, both for single elements and the whole system, was carried out by using numerical procedures based on floating mean regressive processes. The second phase however, includes the dynamic analysis of the model when subjected to different recorded time-history accelerations corresponding to seismic events having very different magnitude and energy content. These input signals have been conveniently scaled with regard to cinematic parameters: time, displacements and accelerations.

Finally, combined strategy effectiveness has been evaluated by comparing the seismic response of the model with and without the application of the mass damper at the isolation layer.

2. SMALL-SCALE MODEL DESCRIPTION

The small-scale model used in the test represents a three degree of freedom system, which can be easily disassembled in three sub-systems (Figure 1), that is:

- Single level framed system, corresponding to the superstructure. This is made up of two steel vertical elements, 50 cm high with a $1.75 \times 101.1 \text{ mm}$ rectangular section, and by a polystyrene horizontal element, 31 cm wide and with a $11 \times 110 \text{ mm}$ section. The framed system has a fundamental vibration period equal to 0,27 sec.;
- Base Isolation system (BIS) made of aluminium material, in order to reduce its weight. It was arranged by using a 6 mm thin supporting plate having significant axial and flexural stiffness; two 14 mm diameter circular rods to allow for the sliding movement of the plate by means of four ball bearings and two dynamometers, acting in parallel, to provide a suitable degree of isolation. BI system presents a fundamental vibration period equal to 0,49 sec.;
- Tuned Mass Damper (TMD) constituted by using a pendulum system with 10% mass ratio. In particular, it is made of a $195 \times 100 \text{ mm}$ aluminium box-shaped element having 4 mm thickness. The oscillating mass consists of a 30 mm cubic element and its position can be modified in order to change the pendulum period in the range 0,28 to 0,77 sec..

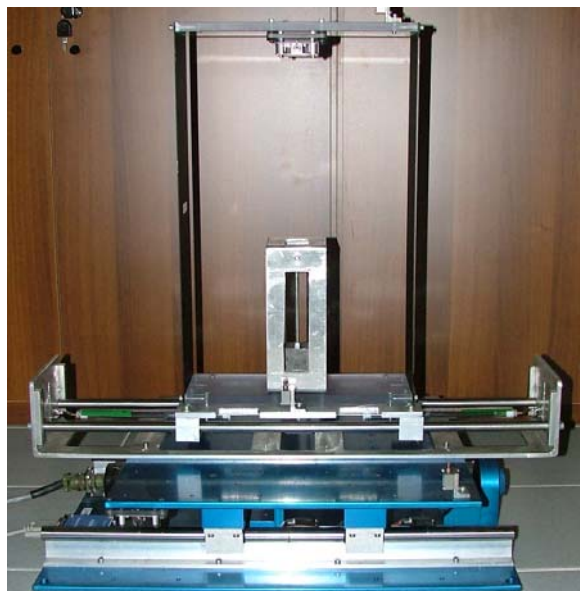


Figure 1: Small Scale Model

In order to provide applicative sense to the experimental results, a cinematic scaling technique has been adopted [Dove and Bennett, 1986], in particular scale ratios for time t and acceleration \ddot{y} have been fixed. It is evident that, scale ratio for length is completely defined by the abovementioned operation:

$$N_t = \bar{N}_t \quad N_{\ddot{y}} = \bar{N}_{\ddot{y}} \quad N_L = \bar{N}_{\ddot{y}} \cdot \bar{N}_t^2 \quad (2.1)$$

where N_t , $N_{\ddot{y}}$ and N_L respectively represent the scale ratio for time, acceleration and length. This approach allows for the study of several real structures, characterized by different fundamental periods, by using the same model and just varying the time scale ratio. Instead, acceleration scale factor controls the shaking table maximum displacement in order to avoid exceeding the physical hardware limit.

It is necessary to observe that the adopted scaling procedure does not allow for any control over the system's damping. Therefore, damping values stay as constant, in particular as equal to 0,90% for the bare framed system and 3,84% for the base isolated one.

3. EXPERIMENTAL SET-UP DESCRIPTION

Experimental tests have been carried out by using a shaking table "Shake Table II" manufactured by "Quanser Consulting" [Dyke and Caicedo, 2002]

The acquisition of the signal data was done by means of a 16 analogue input-channels DAQPad-6015 Board by National Instruments, capable of 16 bit sequential sampling. This hardware allows for capturing signals with a 1000Hz maximum sampling frequency and a $\pm 10V$ width.

During the tests, shaking table, base isolation and framed system accelerations were constantly monitored by using two different accelerometer typologies, whose features are listed in Table 3.1.

Table 3.1: Accelerometer's characteristics

	Quanser	PCB PIEZOTRONICS
Accelerometer	$\pm 5g$	$\pm 3g$
Voltage Sensitivity	1000 mV/g	1000 mV/g (average)
Resolution	0,001 g	0,00003 g

4. IDENTIFICATION PROCEDURE

The first phase of experimentation concerned the dynamic identification of the small-scale model in all its possible configurations. With this aim in mind, the linear dynamic response of the system has been described by using the following mathematical model:

$$y(t) = G(q) \cdot u(t) + H(q) \cdot e(t) \quad (4.1)$$

where $G(q)$ and $H(q)$ represent the system transfer functions relating the dynamic response respectively to the input signal $u(t)$ and the noise $e(t)$, q represents a time-shift math operator defined as follows:

$$q[u(t)] = u(t + \Delta T) \quad \text{and} \quad q^{-1}[u(t)] = u(t - \Delta T) \quad (4.2)$$

where ΔT is the sampling time for the signal $u(t)$.

The two transfer functions $G(q)$ and $H(q)$ were estimated by using an ARMAX (AutoRegressive Moving Average with eXtra input) [Ljung, 1999] procedure, based on a floating mean regressive process. All the computational operations were carried out in Matlab [Ljung, 2007] by using recorded seismic signals.

All sub-systems have been identified by using the ARMAX process and free vibration test and obtained transfer functions positively compared. Figures 2-3 show the results of identification of the system with TMD, whereas figures 4-5 show the effect of different TMD tuning on the systems' frequency response.

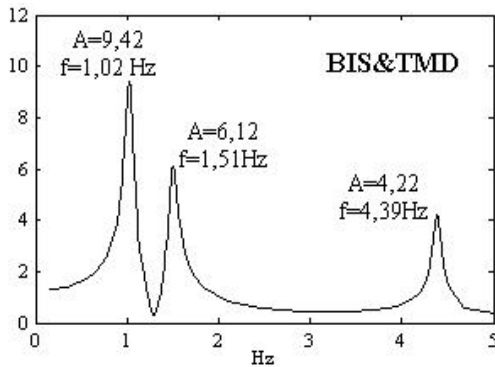


Figure 2: Transfer Function

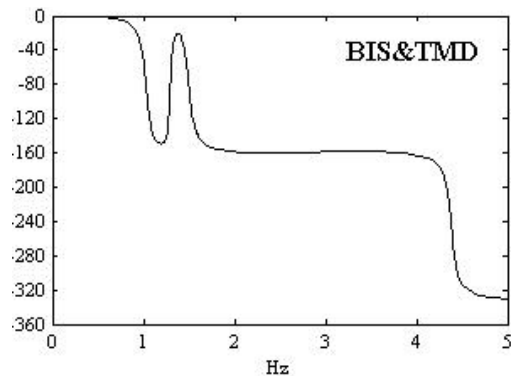


Figure 3: Phase Diagram

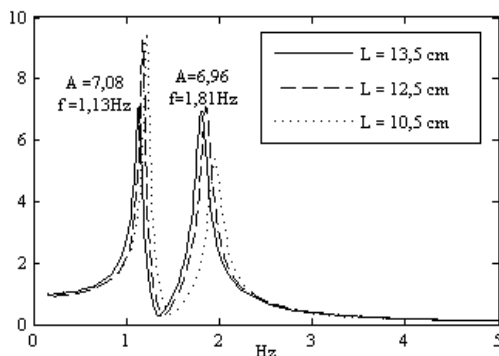


Figure 4: Transfer Function. Effect of TMD tuning

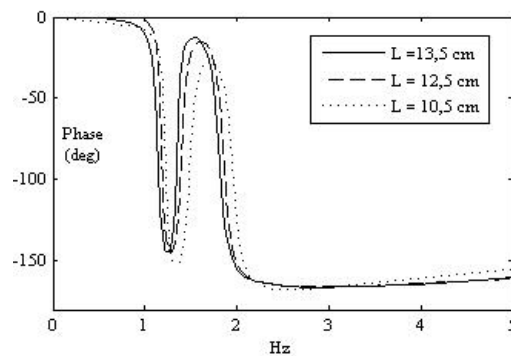


Figure 5: Phase Diagram. Effect of TMD tuning

5. EXPERIMENTAL TEST RESULTS

The small-scale model, in base-isolated configuration with and without TMD, has been tested by using scaled recorded accelerograms, corresponding to seismic events which have taken place in Europe and also used within a National Italian Research Project ReLUI (Rete dei Laboratori Universitari di Ingegneria Sismica).

In Table 5.1, the main features of the considered seismic events are listed, whereas in Table 5.2 the investigated fundamental period range and the corresponding scaling factor for every input signal are reported. In order to numerically investigate a broadest period range for the two most significant seismic events, different values for the parameter N_y are selected. Figures 6-7, 10-11 respectively show the isolation level displacement spectra and the superstructure absolute accelerations spectra with and without TMD, for Belgrade 0199Y and Ankara 0535X seismic events. Figures 8 and 12 show isolation layer relative displacement time-history comparison with and without TMD, while in figures 9 and 13 the same comparison for superstructure acceleration time-histories have been plotted. Results show significant seismic response reduction, in particular isolation level maximum relative displacement decreases from 66.04 cm to 49.66 cm for Ankara 0535X event and from 37.20 cm to 26.04 cm in the case of Belgrade 0199Y earthquake, with a percentage reduction respectively equal to 24,80% and 30,10%.

Table 5.1: Seismic events considered

Seismic events	Date of Reg.	Earth. Cod.	Rec. Time
Belgrade, Yugoslavia	15/04/1979	0196X – 0196Y	48,23 s
Belgrade, Yugoslavia	15/04/1979	0199X – 0199Y	47,82 s
Belgrade, Yugoslavia	15/04/1979	0228X – 0228Y	34,35 s
Italy	23/11/1980	0288X – 0288Y	30,16-73,21 s
Ankara, Turkey	13/03/1992	0535X – 0535Y	21,28 s
Iceland	21/06/2000	6328X – 6328Y	51,37 s

Table 5.2 Scale factors and fundamental period range

Earth. Cod.	T_{BIS}	N_i	N_l	N_v
Belgrade 0196X	1,32 – 1,99	1,78 – 2,67	3,18 – 7,15	1,00
Belgrade 0196Y	0,80 – 2,00	1,07 – 2,69	1,15 – 7,22	1,00
Belgrade 0199X	2,07	2,78	7,74	1,00
Belgrade 0199Y	2,00	2,68	7,19	0,15 – 2,75
Belgrade 0228X	0,74 – 1,33	1,00 – 1,81	1,00 – 3,26	1,00
Belgrade 0228Y	0,74 – 1,33	1,00 – 1,78	1,00 – 3,19	1,00
Enel 0288X	0,46 – 1,99	0,62 – 2,67	0,39 – 7,11	1,00
Enel 0288Y	0,55 – 1,33	0,74 – 1,79	0,54 – 3,20	1,00
Ankara 0535X	3,98	5,34	28,52	0,40 – 5,00
Ankara_0535Y	3,99	5,36	28,71	1,00
Iceland 6328X	0,59 – 2,03	0,80 – 2,73	0,63 – 7,44	1,00
Iceland 6328Y	0,75 – 2,98	1,00 – 2,66	1,00 – 7,09	1,00

It is also important to underline the low sensitivity shown by the superstructure's seismic response to the application of mass damping at the isolation layer.

Figures 14-17 represent the isolation layer relative displacement spectra for seismic inputs allowing for the largest number of experimental tests. These tests have to be considered less significant when compared with the above-mentioned ones. In fact they refer to seismic motion setting slight values for isolation layer relative displacements, because of the seismic energy concentrated in frequencies beyond those fundamental frequencies of the structure. In these cases, the BIS strategy works well and there is no need to use the proposed combined approach.

For instance, if the Iceland 6328X recorded event is considered, in the case of a base-isolated structure having 2,03sec fundamental period, a 18,79% percentage reduction in the maximum relative displacement is observed. However it decreases from 8,09cm to 6,57cm and both values are lower than the admissible maximum relative displacement for a typical base isolation device. Moreover, it should be pointed out that the seismic response of the isolation layer is rarely worsened by the application of a TMD even when BI strategy works well, and that superstructure absolute acceleration is almost always reduced. A rare adverse case is represented by the Belgrade 0196Y seismic excitation, if a base isolated structure with 1,33sec fundamental period is considered the absolute acceleration increases by applying a TMD from 0,18g to 0,28g. However, despite a 50% percentage increase, the base isolation continues to work properly, the absolute acceleration for a fixed-base structure is, in fact, equal to 4,24g.

Finally, Table 5.3 summarises results from the whole experimentation, listing in the first column the accelerogram code, in the second, third and fourth columns respectively the percentage variations of superstructure absolute acceleration due to base isolation strategy ($\Delta\ddot{y}$ % BIS), isolation layer relative displacement (Δy_r % BIS-TMD) due to the application of the TMD and superstructure absolute acceleration ($\Delta\ddot{y}$ % BIS-TMD) still due to the application of the TMD on the isolation level.

Table 5.3 Summary of the experiment results

Cod. Registr.	$\Delta\ddot{y}$ % BIS	Δy_r % BIS-TMD	$\Delta\ddot{y}$ % BIS-TMD	Cod. Registr.	$\Delta\ddot{y}$ % BIS	Δy_r % BIS-TMD	$\Delta\ddot{y}$ % BIS-TMD
Belgrado_0196X	+79.1	+49.63	+12.96	Enel_0288X	+77.12	+2.41	+2.68
Belgrado_0196Y	+82.0	+22.13	-5.75	Enel_0288Y	+61.83	+30.59	+31.23
Belgrado_0199X	+77.3	+54.58	+23.33	Ankara_0535X	+89.47	+1.08	-10.00
Belgrado_0199Y	+72.7	+37.32	+27.27	Ankara_0535Y	+86.89	+14.48	+12.50
Belgrado_0228X	+63.1	+17.55	+0.86	Iceland_6328X	+78.83	+40.99	+8.22
Belgrado_0228Y	+67.7	+10.94	+8.92	Iceland_6328Y	+77.40	+14.41	+17.65

6. CONCLUSION

In the present paper experimental tests on a small-scale model were carried out in order to investigate the applicability of the Base Isolation and Tuned Mass Damping combined control strategy. Previous theoretical studies have proved that this approach allows for protection of the isolation layer from unfavourable seismic events, without reducing the beneficial effects of the Base Isolation strategy to the superstructure dynamic. However, applicational confirmation is required before it should be considered as an applicative real-scale solution.

The results of the experimental tests confirm the effectiveness of the isolation system as a seismic protection technique and show the possibility of improving its robustness by combining this technique with a mass damping passive control strategy. In particular, the seismic response of the isolation layer improve by up 20% in term of maximum relative displacement in the case of earthquake having high energy content on the low frequencies, this reduction can allow the devices to work properly, staying into the displacement limit they are designed for.

Moreover, low sensitivity in the superstructure's seismic response to the application of mass damping at the isolation layer has been observed and the isolation layer seismic response is rarely worsened by the application of a TMD even when BIS strategy works well. The superstructure's absolute acceleration is almost always reduced, and even when it increases the seismic isolation continues to work in an effective way.

REFERENCES

- Palazzo B., Petti L. (1994). Seismic Response Control in Base Isolated System using Tuned Mass Dampers, *Proceedings of First World Conference on Structural Control*, August 3-5, Los Angeles, California
- Dove R.C., Bennet J. G. (1986). Scale Modeling of Reinforced Concrete Category I Structures Subjected to Seismic Loading. *Mechanical/Structural Engineering Branch Division of Engineering Technology Office of Nuclear Regulatory Research U.S. Nuclear Regulatory Commission*, Washington, DC 20555.
- Dyke S.J., Caicedo J.M. (2002), The University Consortium on Instructional Shake Tables, *Proceedings of the ICANCEER Conference*, Harbin, China, August 15–20, 2002.
- L. Ljung (1999). *System Identification: Theory for the User*, II edition. Prentice Hall, Upper Saddle River, N.J.
- L. Ljung (2007). *System Identification Toolbox 7 User's Guide*, Revised for Version 7.1 (Release 2007b), The MathWorks, Inc.

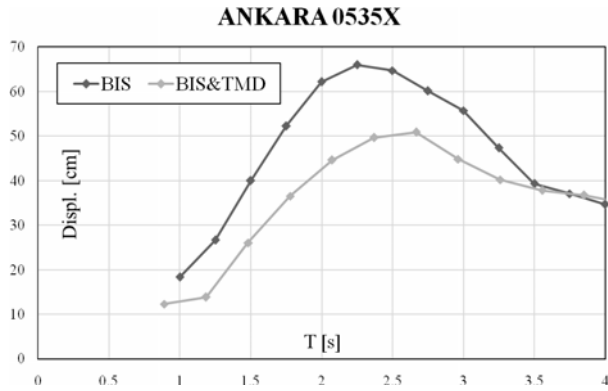


Figure 6: Isolation level relative displacement spectra

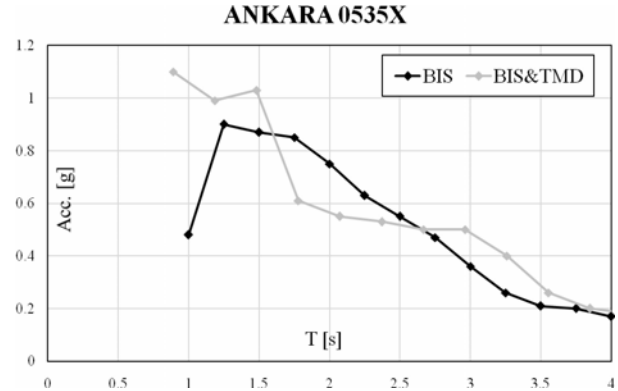


Figure 7: Superstructure absolute acceleration spectra

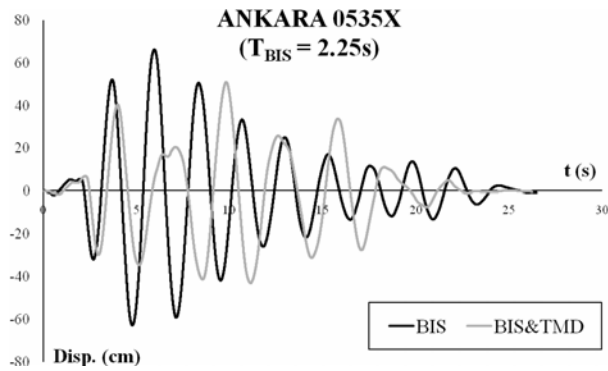


Figure 7: Isolation level relative displacement time history

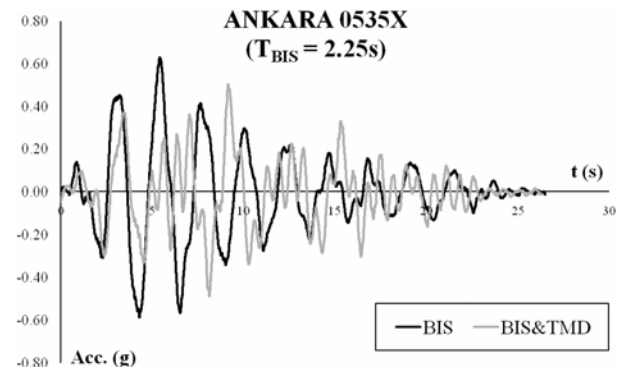


Figure 8: Superstructure absolute acceleration time history

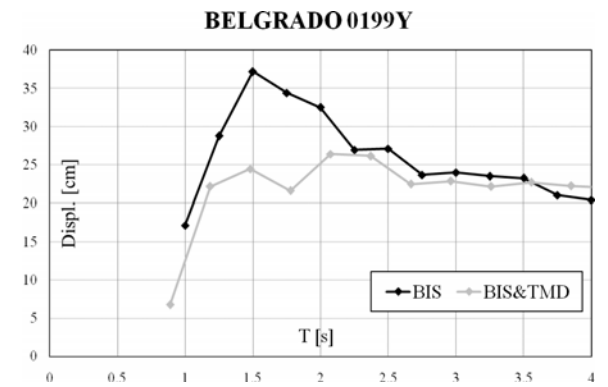


Figure 10: Isolation level relative displacement spectra

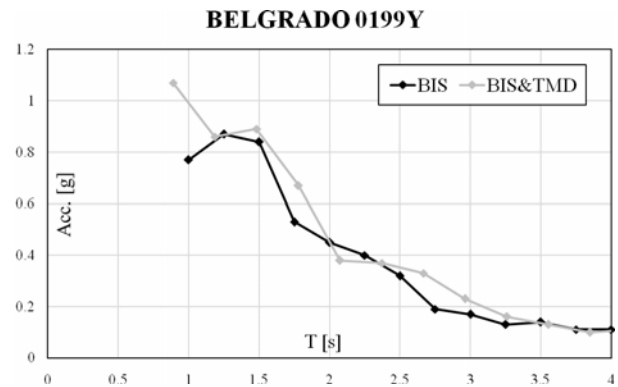


Figure 11: Superstructure absolute acceleration spectra

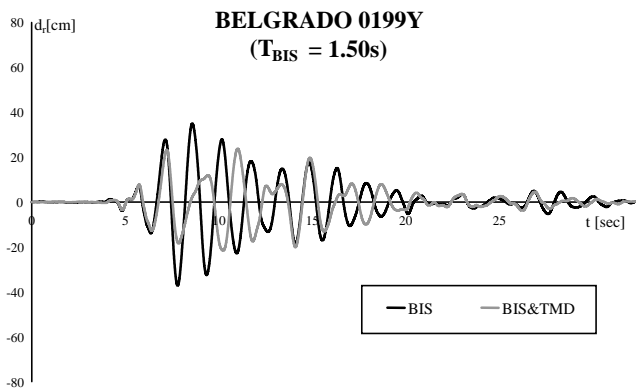


Figure 12: Isolation level relative displacement time history

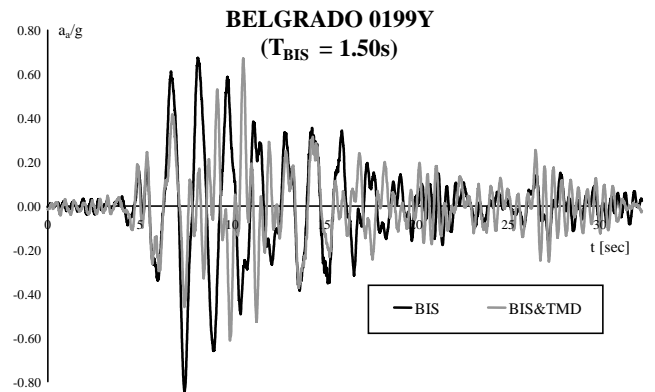


Figure 13: Superstructure absolute acceleration time history

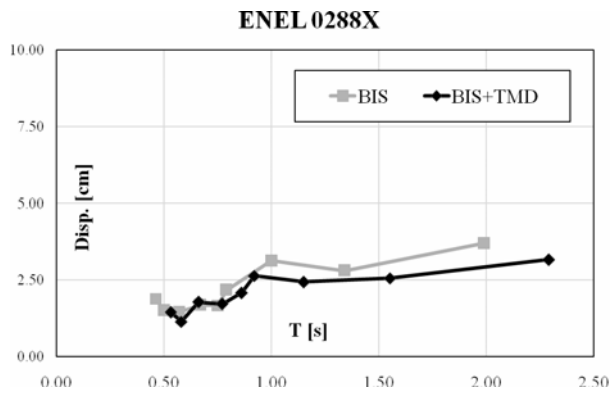


Figure 14: Isolation level relative displacement spectra

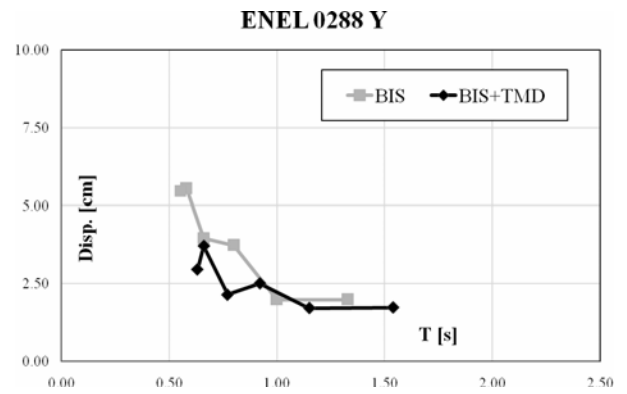


Figure 15: Isolation level relative displacement spectra

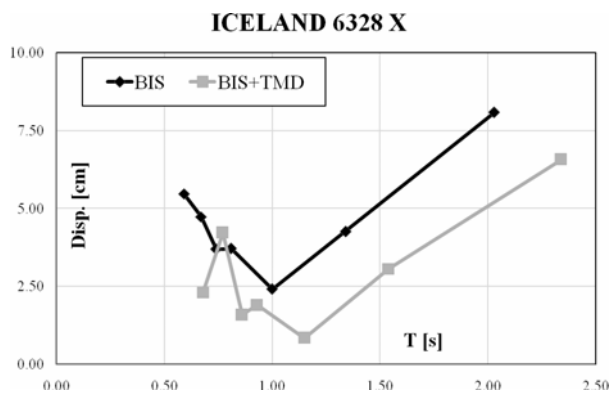


Figure 16: Isolation level relative displacement spectra

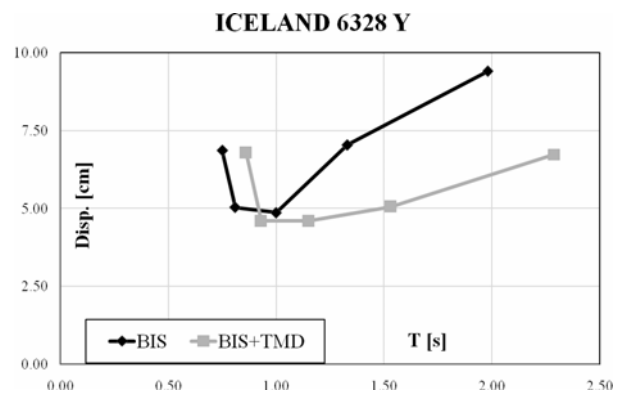


Figure 17: Isolation level relative displacement spectra